$PDMS_{STAR}$-PEG HYDROGELS FOR OSTEOCHONDRAL TISSUE ENGINEERING

An Undergraduate Research Scholars Thesis

by

ERICA GACASAN

Submitted to Honors and Undergraduate Research
Texas A&M University
in partial fulfillment of the requirements for the designation of

UNDERGRADUATE RESEARCH SCHOLAR

Approved by
Research Advisor: Dr. Melissa Grunlan

May 2014

Major: Biomedical Engineering

TABLE OF CONTENTS

Page

ABSTRACT 1

DEDICATION 3

ACKNOWLEDGEMENTS 4

NOMENCLATURE 5

CHAPTER

I. INTRODUCTION 6

II. METHODS 9

Materials 9

Methods 9

III. RESULTS 14

Hydrogel Fabrication 14

Hydrogel Morphology 15

Equilibrium Swelling 16

Modulus 17

Degradation 18

IV. CONCLUSION 20

REFERENCES 21

ABSTRACT

PDMS$_{star}$-PEG Hydrogels for Osteochondral Tissue Engineering. (May 2014)

Erica Gacasan
Biomedical Engineering
Texas A&M University

Research Advisor: Dr. Melissa Grunlan
Department of Biomedical Engineering

Tissue engineering may utilize a "materials-guided" approach to repair of osteochondral defects (OCDs) – damage extending from cartilage to subchondral bone. Based on the physical and chemical properties of the scaffold alone, cell behavior may be directed to regenerate tissues in a spatially controlled geometry. Conventional poly(ethylene glycol) diacrylate (PEG-DA) hydrogels, prepared via photocure of aqueous precursor solutions, have been extensively studied as instructive scaffolds. However, due to a somewhat narrow range of properties and a lack of bioactivity and osteoinductivity, PEG-DA hydrogels require modification in order to promote osteochondral regeneration. Towards this goal, three fabrication parameters were systematically studied. First, methacrylated star polydimethylsiloxane (PDMS$_{star}$-MA) was introduced with PEG-DA to induce the formation of hydroxyapatite (i.e. for bioactivity) and to promote mesenchymal stem cell (MSC) lineage progression towards osteoblast-like fates (i.e. for osteoinductivity). Second, solvent induced phase separation (SIPS), involving an organic fabrication solvent, was employed in lieu of a conventional aqueous fabrication solvent. Lastly, interconnected pores were introduced and tailored through a modified solvent-casting/particulate leaching (SCPL) technique in conjunction with SIPS. The influence of total macromer concentration, weight percent (wt%) ratio of PDMS$_{star}$-MA to PEG-DA and average salt particle

size on bioactivity, morphology, hydration, degradation, and mechanical properties was evaluated.

DEDICATION

To my parents.

ACKNOWLEDGEMENTS

I would like to thank my advisor Dr. Melissa Grunlan for allowing me the chance to partake in the research herein, and for her guidance and support throughout this journey. I would also like to thank her graduate students Dr. Brennan Bailey, Lindsay Nail, and Raymond Fei, as well as fellow undergraduate student researchers Rebecca Sehnert and Berkay Başağaoğlu for their efforts and support.

Thanks also to the Office of Undergraduate Research for their assistance provided in correcting and finalizing this thesis. Financial support from the Department of Honors and Undergraduate Research, the Aggie Research Scholars Program, as well as the George Bush Presidential Library Foundation is gratefully acknowledged.

Finally, thank you to my friends and family for their reassurance and encouragement in my life and throughout my studies, pushing me always to raise the bar.

NOMENCLATURE

DCM	Dichloromethane
G’	Compressive storage modulus
MSC	Mesenchymal stem cell
OCD	Osteochondral defect
PEG-DA	Poly(ethylene glycol) diacrylate
$PDMS_{star}$-MA	Methacrylated star polydimethylsiloxane
RT	Room temperature
SCPL	Solvent-casting/particulate leaching
SIPS	Solvent induced phase separation
wt%	Weight percent

CHAPTER I

INTRODUCTION

Osteochondral defects (OCDs) - damage that extends from cartilage to subchondral bone - is a major cause of disability around the world [1, 2]. Due to the limited vasculature associated with articular cartilage, OCDs are limited in their ability to heal themselves and the condition progresses [3]. Tissue engineering represents a promising alternative to heal OCDs. "Materials-guided" tissue engineering utilizes an instructive scaffold whose physical and chemical properties alone (e.g. without exogenous growth factors) direct cell behavior [4-6]. Through the modulation of scaffold properties, regeneration of tissues with properties similar to those of native tissue may be ultimately achieved [6]. Notable is the interfacial nature of osteochondral tissue which provides mechanical support and functionality to the cartilage [3]. Thus, to regenerate osteochondral tissues, the instructive osteochondral scaffold should ideally be comprised of a continuous gradient of both physical properties (e.g. morphology or porosity, and modulus) and chemical properties (e.g. chemical functionality, hydrophobicity, hydration, and bioactivity) that can spatially direct cell behavior. Towards this goal, a library of scaffolds which may appropriately guide cell behavior and can be formed as continuous gradients are needed.

Poly(ethylene glycol) diacrylate (PEGD-DA) hydrogels have been widely utilized for materials-guided tissue engineering due to their utility as a "biological blank slates" [7, 8]. Thus, due to their inherent resistance to protein and cell adhesion, cell adhesion is accomplished in a controlled fashion. This has rendered PEG-DA hydrogels particularly useful for the investigation of cell-material interactions towards tissue regeneration. However, PEG-DA hydrogels are

limited by a lack of osteoinductivity and bioactivity, as well as a somewhat narrow range of tunable physical properties [7]. For instance in PEG-DA scaffolds, modulus can be tuned somewhat by varying crosslink density and weight % concentration [4, 7, 9]. However, these changes produce a concomitant change in swelling, restricting the ability to independently study modulus and swelling.

Previously, hybrid inorganic-organic PEG hydrogels were fabricated with methacrylated star polydimethylsiloxane ($PDMS_{star}$-MA) using a conventional aqueous fabrication solvent [10]. The resultant hydrogel compositions broadened the range of chemical and physical properties versus that of conventional PEG-DA hydrogels. Moreover, the incorporation of $PDMS_{star}$-MA, an inorganic and hydrophobic material, was shown to enhance bioactivity and induce osteogenic differentiation of mesenchymal stem cells (MSCs) in proportion to $PDMS_{star}$-MA content [10]. $PDMS_{star}$-PEG hybrid scaffolds were also prepared via solvent induced phase separation (SIPS). SIPS $PDMS_{star}$-PEG hydrogels exhibited enhanced pore size, modulus, degradation rates and, at times, morphology and hydration were uncoupled [4]. SIPS fabricated hydrogels also featured a more homogenous distribution of $PDMS_{star}$-MA versus the analogous conventional hydrogel [4]. Finally, SIPS $PDMS_{star}$-PEG scaffolds were prepared as continuous gradients with, for instance, a gradual transition in PDMS concentration [9].

Although SIPS $PDMS_{star}$-PEG hydrogels exhibit enhanced pore size, they lack the pore interconnectivity critical to facilitating cell infiltration into the scaffold, tissue integration, and diffusion of nutrients and cellular waste products. As such, macroporous hydrogels with interconnected pores have been shown to be particularly useful in tissue regeneration by

mimicking the properties of native extracellular matrix (ECM) [11-14]. The optimal pore size varies between desired cell and tissue types. For example, the optimal pore size for cartilage is about 100-200 μm [15] and 100-450 μm for bone [15, 16]. Therefore, strategies such as gas foaming [17], cryogelation [18, 19], and particulate leaching [12, 13] have been investigated for the controlled introduction of macroporous architecture into PEG-DA hydrogels.

Particulate leaching provides an opportunity to finely tune pore size and pore interconnectivity [20]. Even so, investigations into particulate leaching in PEG-DA hydrogels have been limited due to the soluble nature of porogens (e.g. salt and sugar) in the aqueous fabrication solvent [12, 13]. However, by combining SIPS, which uses an organic fabrication solvent, solvent-casting/particulate leaching (SCPL) can be used to introduce desired pore features into $PDMS_{star}$-PEG hydrogels. In this work, we sought to enhance the utility of PEG-DA hydrogels as instructive osteochondral scaffolds through the integration of three fabrication parameters. First, $PDMS_{star}$-MA was incorporated to enhance bioactivity and osteoinductivity. Second, a SIPS protocol was employed in place of conventional aqueous fabrication. Lastly, pore interconnectivity was tailored through SCPL techniques. Distinct salt-leached hybrid scaffolds were prepared in which the total macromer concentration and wt% ratio of $PDMS_{star}$-MA to PEG-DA was studied with regard to their impact on scaffold morphology, hydration, mechanical properties, and degradation rate.

CHAPTER II

METHODS

Materials

Octamethylcyclotetrasiloxane (D_4), Pt-divinyltetramethyldisiloxane complex (Karstedt's Catalyst, 2 wt% in xylene), and tetrakis(dimethylsiloxy)silane (tetra Si-H) were obtained from Gelest. 1-Vinyl-2-pyrrolidinone (NVP), 2,2-dimethyl-2-phenyl-acetophenone (DMAP), dichloromethane (DCM), acryloyl chloride, allyl methacrylate, hexamethyldisilazane (HMDS), $MgSO_4$, K_2CO_3, NaCl, NaOH, triethyl amine (Et_3N), and triflic acid were obtained from Sigma Aldrich. Poly(ethylene glycol) (PEG; MW=3000-3700 g mol^{-1} per manufacturer's specifications) were obtained from BioChemika.

Methods

$PDMS_{star}$-MA Synthesis

$PDMS_{star}$-MA (7k g mol^{-1}) was prepared as previously reported [10, 21].

PEG-DA Synthesis

PEG-DA (3.4k g mol^{-1}) was prepared as previously reported [10]. By ^{1}H-NMR end-group analysis, the M_n of PEG-DA (3.4k g mol^{-1}) was determined to be 3393 g mol^{-1} (~3400 g mol^{-1}).

NMR

^{1}H-NMR spectra were obtained on a Mercury 300 300 MHz spectrometer operating in the Fourier transform mode. Five percent (w/v) $CDCl_3$ solutions were used to obtain spectra. Residual $CHCl_3$ served as an internal standard.

Hydrogel Preparation

NaCl particles were sieved through an opening of 425 µm to a salt size of 459 ± 69 µm. The average size of each group was determined from SEM images with ImageJ® software (http://rsb.info.nih.gov/ij/).

To prepare a planar salt template, a silicon well (20 × 20 × 1.5 mm) was clamped to a microscope slide (75 × 50 mm). To this well space was added 3.75 g of a NaCl/water mixture (5 wt% water based on NaCl weight) and distributed evenly across the surface. A second glass slide was placed on top, slightly offset as to allow a slight opening for later solution delivery via syringe, and the entire mold structure secured with binder clips. The salt template was then dried at room temperature (RT) in a vacuum oven (14.7 psi, 24 h).

DCM-based precursor solutions were utilized to produce SIPS $PDMS_{star}$-PEG hydrogels. DCM-based precursor solutions were prepared with total macromer concentrations of 20, 30, 40, 50, and 60 wt%. For each concentration, wt% ratios of 0:100 and 20:80 ($PDMS_{star}$-MA to PEG-DA) were utilized. Per 1 ml of each macromer solution was added 10 µl of photoinitiator solution (30 wt% DMAP in NVP). The resulting precursor solutions were vortexed for 1 minute following addition of each component.

A given precursor solution was injected into the mold via syringe so as to cover the salt template. The mold was then exposed to longwave UV light (UV-transilluminator, 6 mW cm^{-2}, 365 nm) for 6 min, with rotation to the alternate side after 3 min. After removal from the mold, the DCM/salt-containing hydrogel sheets were thoroughly rinsed with deionized (DI) water (5 min). DCM and salt were leached from the hydrogel by subsequently soaking a sheet in a Petri dish containing DI water (60 ml) for 72 h, with twice daily water changes.

Sol Content

Three discs (13 mm diameter) were punched from a single hydrogel sheet with a die. After gently blotting the surface with a Kim wipe, each disc was placed in an open 20 ml scintillation vial and dried at RT in a vacuum oven (14.7 psi, 24 h). Dried discs were sequentially weighed (W_{d1}), placed in a new vial, 10 ml of DCM added to each, the vials capped, and then placed on a rocker table (250 rpm) for 48 h to remove sol (e.g. uncrosslinked material). The discs were then removed, air dried for 30 min, placed in an open vial, dried at RT in a vacuum oven (14.7 psi, 24h) and weighed (W_{d2}). The sol content is defined as $[(W_{d1}-W_{d2})/W_{d1}] *100$.

Scanning Electron Microscopy (SEM)

Water-swollen hydrogels discs (13 mm diameter) were flash frozen in liquid nitrogen for 1 min and immediately lyophilized for 24 h (Labconco Centri Vap Gel Dryer System). Specimen cross-sections were subjected to Pt-sputter coating and viewed with a field emission scanning electron microscope (JEOL 6400 SEM) at an accelerated electron energy of 10 keV.

Equilibrium Swelling

Three discs (13 mm diameter) were punched from each of three hydrogel sheets (n = 9) with a die. Each disc was placed in a sealed vial containing 20 ml of DI water and placed on a rocker table (250 rpm) for 48 hr at RT. Discs were then removed from water and weighed (W_s). Subsequently, the water-swollen hydrogel was blotted with filter paper and dried in a vacuum oven (14.7 psi, 60 °C, 24 h). The equilibrium swelling ratio (SR) is defined as $(W_s - W_d)/W_d$, where W_s is the weight of the water-swollen hydrogel and W_d is the weight of the vacuum dried hydrogel.

Dynamic Mechanical Analysis (DMA)

Nine discs (13 mm diameter) were prepared as above. The compressive storage modulus (G') of each disc was measured in the compression mode using a dynamic mechanical analyzer (TA Instruments Q800) equipped with a parallel-plate compression clamp with the diameters of 40 mm (bottom) and 15 mm (top). A water-swollen disc (13 mm diameter) was clamped between the parallel plates. Following equilibration at 25 °C (5 min), the samples were tested in a multi-frequency strain mode (1–30 Hz).

Degradation

Six hydrogel discs (8 mm diameter) were punched from a hydrogel sheet with a dye. After soaking in DI water for 3 h, the initial swollen weight (W_s) was recorded. Three discs were each placed into a well of a 24-well plate containing 1 ml 0.05 M NaOH, the well plate covered with Parafilm and maintained at 37 °C on a rocker table at 50 rpm. The NaOH solution was exchanged every 12 h. Swollen weights (W_s) were recorded at regular intervals until the

hydrogel exhibited an increase in swelling with a corresponding loss in mechanical integrity. The time required for the disc to completely dissolve was also recorded. The remaining three hydrogel discs were vacuum dried (14.7 psi, 60 °C, 24 h) and their weights recorded (W_d). The SR is defined as above.

CHAPTER III

RESULTS

Hydrogel Fabrication

SIPS $PDMS_{star}$-PEG hydrogels with interconnected pores were prepared using a modified SCPL protocol to achieve control over pore features. With this strategy, pore size may be readily controlled with salt particle size and pore interconnectivity affected via addition of small quantities of water to fuse the salt template [22, 23]. Previously, it was noted that addition of 5 wt% water to NaCl particles (459 ± 69 μm) effectively produced an interconnected template [20]. Thus, in this work, we utilized these parameters to produce interconnected pores with sizes shown to improve bone regeneration [15, 16]. To afford control over the chemical and physical properties of SIPS $PDMS_{star}$-PEG hydrogels, DCM-based precursor solutions added to the salt template were prepared with varying levels of total macromer concentrations (20, 30, 40, 50, and 60 wt%) and with both a 0:100 and 20:80 wt% ratio ($PDMS_{star}$-MA to PEG-DA) for each. Following leaching of the salt template, the hydrogels' porous structure was visible under normal light (Figure 1). While hydrated porated SIPS PEG-DA hydrogels were transparent, SIPS $PDMS_{star}$-PEG SIPS hydrogels appeared slightly opaque. Hydrogel sol content values were measured to evaluate the efficacy of photocrosslinking. The sol content values of hydrogels fabricated without PDMS (~1-3%) and with PDMS (~3-13%) were similarly low.

a) Salt Mold b) Salt Containing Gel c) Final Gel

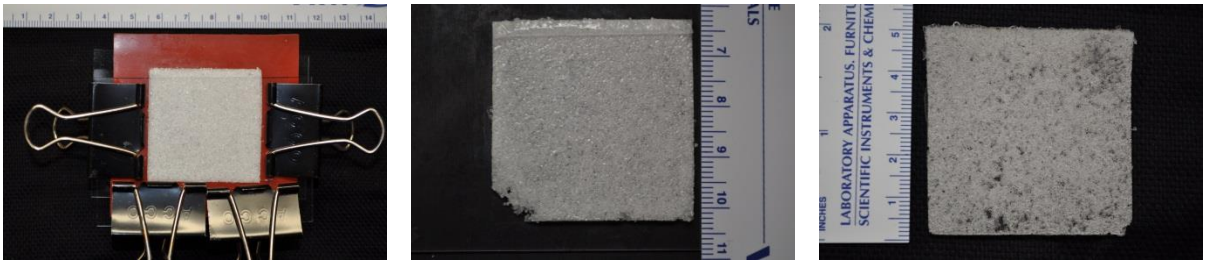

Figure 1: Fabrication of porated $PDMS_{star}$-PEG hydrogels using a modified SCPL technique in conjunction with SIPS. a) Template of fused salt crystals. b) Salt-containing hydrogel sheet following UV cure. c) Final hydrogel sheet after leaching of salt template.

Hydrogel Pore Morphology

Previously, it was observed that SIPS $PDMS_{star}$-PEG hydrogels (e.g. fabricated with a DCM precursor solution) exhibited enhanced pore size with increased $PDMS_{star}$-MA content [4]. During SIPS, porosity is produced by separation of the growing polymer chains and network from the solvent into polymer-rich and polymer-lean domains, thereby producing large pores.

In this work, SEM was used to characterize and examine pore morphologies of SIPS $PDMS_{star}$-PEG hydrogels (Figure 2). SEM images of the hydrogel cross-section illustrate a high degree of porosity and the presence of an interconnected pore network in both pure PEG-DA and hybrid $PDMS_{star}$-PEG hydrogels. In contrast, non-porated SIPS hydrogels lack such interconnectivity [4]. In addition, pore walls have a "microporated" appearance, perhaps due to the nature of the SIPS fabrication process.

a) 20 wt% PURE

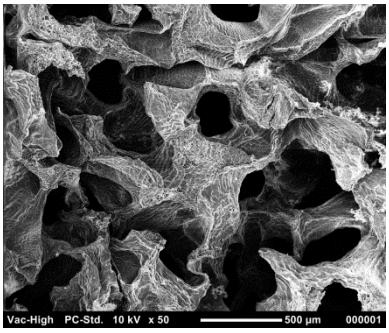

b) 20 wt% (20:80)

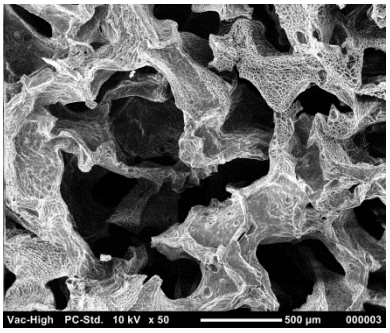

c) 20 wt% (20:80)

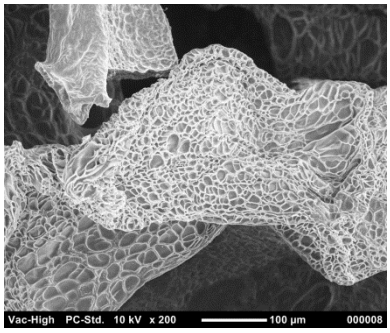

Figure 2: SEM images showing effect of $PDMS_{star}$-MA on pore morphology. a) Pure PEG-DA hydrogel of 20 wt% total macromer concentration, bar indicates 500µm. b) $PDMS_{star}$- PEG (20:80) hydrogel of 20 wt% total macromer concentration, bar indicates 500 µm. c) Microporatio of $PDMS_{star}$-MA:PEG-DA (20:80) hydrogel of 20 wt% total macromer concentration, bar indicates 100 µm.

Equilibrium Swelling

The water content of the hydrogel scaffold will impact both the cellular environment as well as diffusion of cellular wastes and nutrients [24, 25]. Equilibrium swelling studies were performed to examine the difference between porated PEG-DA and $PDMS_{star}$-PEG SIPS hydrogels (Figure 3). In spite of enhanced levels of hydrophobic $PDMS_{star}$-MA, $PDMS_{star}$-PEG-DA hydrogels exhibited enhanced swelling versus the corresponding PEG-DA hydrogels. This may be attributed to enhanced levels of phase separation.

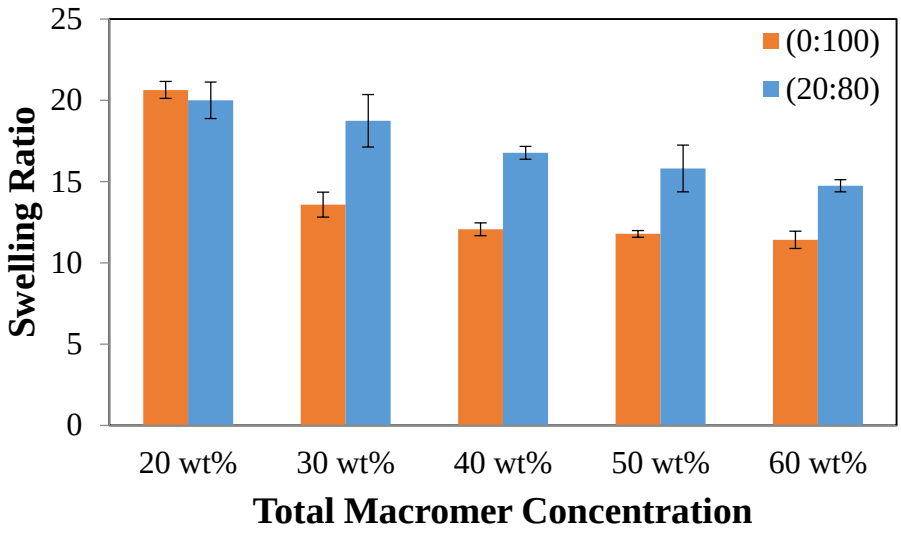

Figure 3: Swelling ratio of porated $PDMS_{star}$-PEG hydrogels formed with 0:100 and 20:80 wt% ratio ($PDMS_{star}$-MA:PEG-DA), respectively.

Modulus

Scaffold stiffness is known to impact cell behavior [25]. Using DMA, G' was measured as a function of frequency (Figure 4). For a given total wt%, G' was substantially higher for porated SIPS PEG-DA hydrogels versus the corresponding porated $PDMS_{star}$-PEG hydrogel. This may be attributed to the enhanced swelling of the latter. As expected [7], an increase in the total wt% macromer concentration produced a concomitant increase in G'.

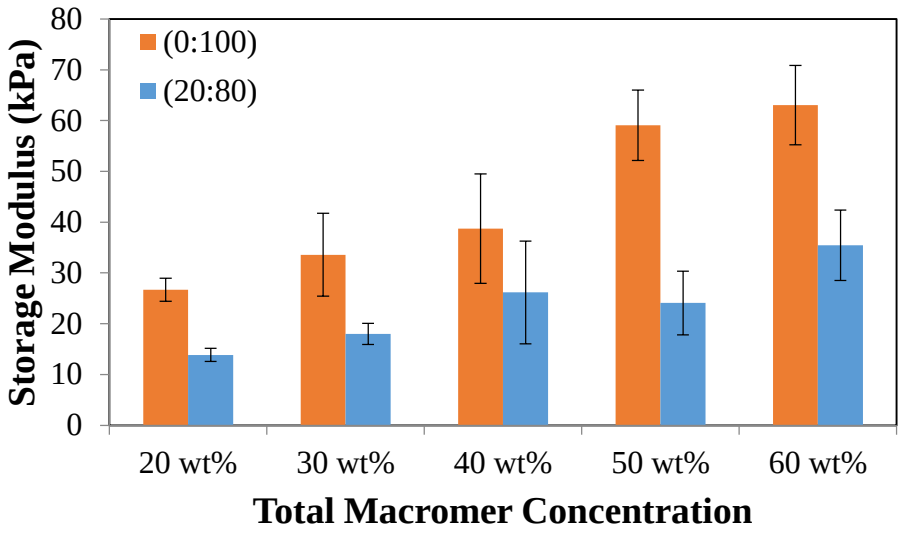

Figure 4: Storage modulus of porated SIPS PEG-DA and $PDMS_{star}$- PEG hydrogels formed with 0:100 and 20:80 wt% ratio ($PDMS_{star}$-MA to PEG-DA), respectively.

Degradation

The rate of scaffold degradation should parallel the rate of tissue regeneration for optimal healing. Thus, all samples were subjected to hydrolytic degradation under accelerated (basic) conditions, where degradation was measured as a function of swelling until a loss of mechanical integrity occurred (Figure 5). In addition, the time required for complete dissolution was also recorded. For aliphatic polyesters, the rate of hydrolytic degradation increases with larger pore size, because of the associated greater pore wall thickness, due to an autocatalytic effect of more slowly diffusing acidic degradation products [26, 27]. In addition, for PEG-DA hydrogels, hydrolysis of labile ester bonds releases poly(acrylic acid) (PAA) kinetic chains which induce autoacceleration [28]. Thus, the initial enhanced rate of degradation of hybrid SIPS $PDMS_{star}$-PEG-DA hydrogels versus pure PEG hydrogels is attributed to the latter's enhanced porosity. However, at higher wt% total concentrations the enhanced degradation rate of hybrid $PDMS_{star}$-PEG hydrogels was mitigated by increasing hydrophobicity. Therefore, as previously reported,

degradation rate is determined both by enhanced hydrophobicity and porosity [4]. As expected, degradation rate was also found to decrease with increased total wt% macromer concentration.

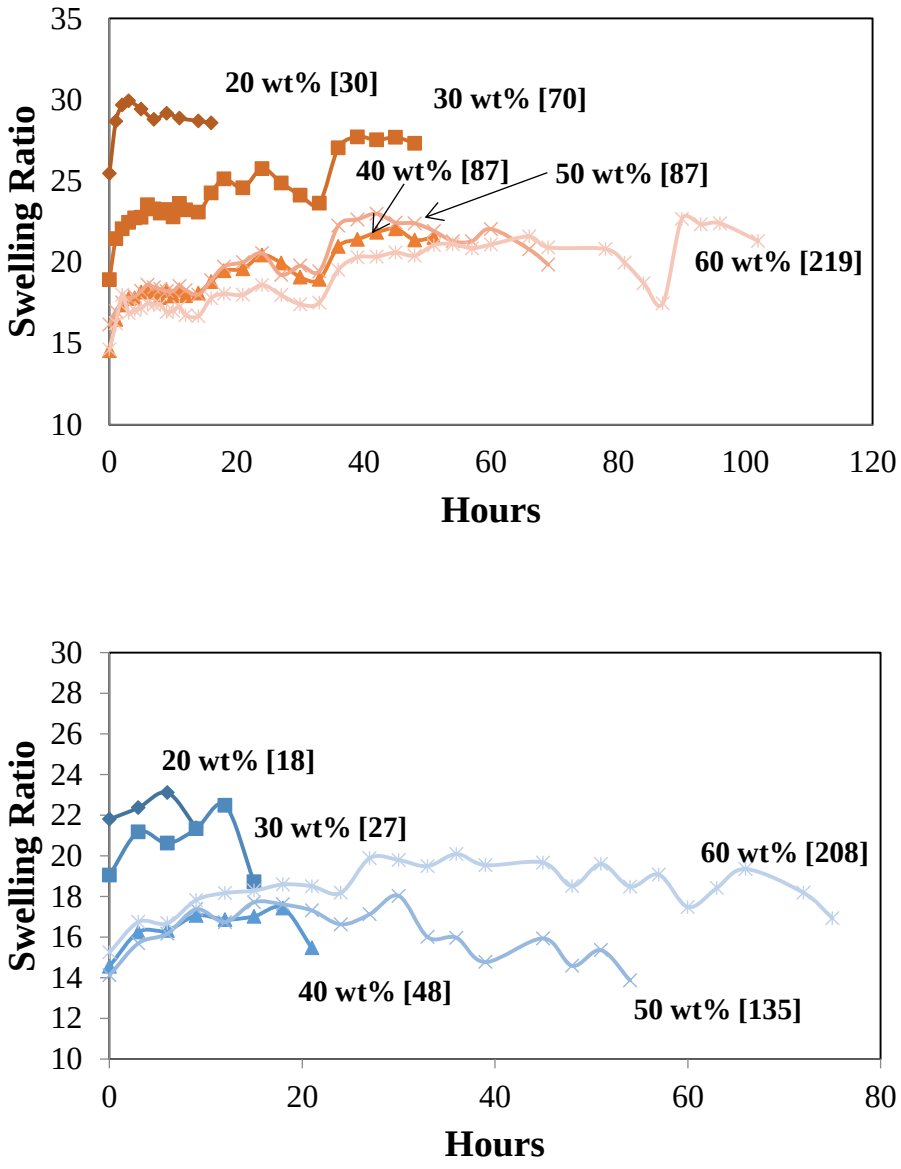

Figure 5: Swelling ratio under basic conditions (0.05M NaOH) of porated SIPS hydrogels formed with 0:100 (top) and 20:80 (bottom) wt% ratio ($PDMS_{star}$-MA:PEG-DA); [ ] = hours to complete dissolution.

CHAPTER IV

CONCLUSION

PEG-DA scaffolds with enhanced bioactivity and osteoinductivity as well as pore interconnectivity would be useful in the development of a hydrogel scaffold for regeneration of osteochondral tissues. Thus, porated inorganic-organic $PDMS_{star}$-PEG hydrogels were prepared using SCPL in conjunction with SIPS to create a bioactive, osteoinductive and highly interconnected porous matrix. Upon the incorporation of $PDMS_{star}$-MA, fabricated hydrogels exhibited enhanced swelling, degradation, and reduced modulus versus the corresponding PEG-DA hydrogel. However, nanoindentation would be useful to determine local modulus versus "net" modulus of these porated SIPS hydrogels [29, 30] to more accurately assess the local cell environment. Incorporation of pluripotent cells (e.g. MSCs) into $PDMS_{star}$-PEG scaffolds would provide an understanding of possible cell-material interactions and augment the scaffold library available to direct potential osteochondral healing.

REFERENCES

[1] Brooks P. The burden of musculoskeletal disease- a global perspective. Clin Rheumatol 2006;25:778-81.

[2] C. Niek van Dijk, Reilingh M, Zengerink M, Bergen Cv. Osteochondral defects in the ankle: why painful? Knee Surg Sports Traumatol Arthrosc 2010;18:570-80.

[3] Gao J, Dennis JE, Solchaga LA, Goldberg VM, Caplan AI. Repair of osteochondral defect with tissue-engineered two-phase composite material of injectable calcium phosphate and hyaluronan sponge. Tissue Eng 2002;8:827-37.

[4] Bailey BM, Fei R, Munoz-Pinto D, Hahn MS, Grunlan MA. PDMSstar–PEG hydrogels prepared via solvent-induced phase separation (SIPS) and their potential utility as tissue engineering scaffolds. Acta Biomaterialia 2012;8:4324-33.

[5] Keskar V, Marion NW, Mao JJ, Gemeinhart RA. In vitro evaluation of macroporous hydrogels to facilitate stem cell infiltration, growth, and mineralization. Tissue Eng Part A 2009;15:1695-707.

[6] Ziats NP, Miller KM, Anderson JM. In vitro and in vivo interactions of cells with biomaterials. Biomaterials 1988;9:5-13.

[7] Bailey BM, Hui V, Fei R, Grunlan MA. Tuning PEG-DA hydrogel properties via solvent-induced phase separation (SIPS). J Mater Chem 2011;21:18776-82.

[8] Choi HG, Zhang Z, Bocazzi P, Laibinis PE, Sinskey AJ, Jensen KF. Poly(ethylene glycol) (PEG)- modified poly(dimethylsiolxane) (PDMS) for protein and cell-resistant surfaces in microbioreactor. 7th lnt'l Conf Min Chem Biochem Anal Sys. Squaw Valley, Callfornla USA2003. p. 1105-8.

[9] Bailey BM, Nail LN, Grunlan MA. Continuous gradient scaffolds for rapid screening of cell-material interactions and interfacial tissue regeneration. Acta Biomaterialia 2013;9:8254-61.

[10] Hou Y, Schoener CA, Regan KR, Munoz-Pinto D, Hahn MS, Grunlan MA. Photo-cross-linked $PDMS_{star}$-PEG hydrogels: synthesis, characterization, and potential application for tissue engineering scaffolds. Biomacromolecules 2010;11:648-56.

[11] Brauker JH, Carr-Brendel VE, Martinson LA, Crudele J, Johnston WD, Johnson RC. Neovascularization of synthetic membranes directed by membrane microarchitecture. J Biomed Mater Res 2004;29:1517-24.

[12] Chen C-W, Betz MW, Fisher JP, Paek A, Chen Y. Macroporous hydrogel scaffolds and their characterization by optical coherence tomography. Tissue Eng Part C 2011;17:101-12.

[13] Chiu Y-C, Larson JC, Isom A, Brey EM. Generation of porous poly(ethylene glycol) hydrogels by salt leaching. Tissue Eng Part C 2010;16:905-12.

[14] Hollister SJ. Porous scaffold design for tissue engineering. Nat Mater 2005;4:518-24.

[15] Duan P, Pan Z, Cao L, He Y, Wang H, Qu Z, et al. The effects of pore size in bilayered poly(lactide-co-glycolide) scaffolds on restoring osteochondral defects in rabbits. J Biomed Mater Res Part A 2013;102:180-92.

[16] Gong Y, Ma Z, Gao C, Wang W, Shen J. Specially elaborated thermally induced phase separation to fabricated poly(L-lactic acid) scaffolds with ultra large pores and good interconnectivity. J Appl Polym Sci 2006;101:3336-42.

[17] Sannino A, Netti PA, Madaghiele M, Coccoli V, Luciani A, Maffezzoli A, et al. Synthesis and characterization of macroporous poly(ethylene glycol)-based hydrogels for tissue engineering application. J Biomed Mater Res Part A 2006;79A.

[18] Hwang Y, Sangaj N, Varghese S. Interconnected macroporous poly(ethylene glycol) cryogels as a cell scaffold for cartilage tissue engineering. Tissue Eng Part A 2010;16:3033-41.

[19] Hwang Y, Zhang C, Varghese S. Poly(ethylene glycol) cryogels as potential cell scaffolds: effect of polymerization conditions on cryogel microstructure and properties. J Mater Chem 2009;20:345-51.

[20] Zhang D, Burkes WL, Schoener CA, Grunlan MA. Porous inorganic-organic shape memory polymers. Polymer 2012;53:2935-41.

[21] Grunlan MA, Lee NS, Mansfeld F, Kus E, Finlay JA, Callow JA, et al. Minimally adhesive polymer surfaces prepared from star oligosiloxanes and star oligofluorosiloxanes. J Polym Sci Part A: Polym Chem 2006;44:2551-66.

[22] Mikos AG, Thorsen AJ, Czerwonka LA, Bao Y, Langer R. Preparation and characterization of poly(L-lactic acid) foams. Polymer 1994;35:1068-77.

[23] Yang S, Leong K-F, Du Z, Chua C-K. The design of scaffolds for use in tissue engineering. Part I. Traditional factors. Tissue Eng 2001;7:679-89.

[24] Drury JL, Mooney DJ. Hydrogels for tissue engineering: scaffold design variables and applications. Biomaterials 2003;24:4337-51.

[25] Kirschner CM, Anseth KS. Hydrogels in healthcare: from static to dynamic material microenvironments. Acta Materialia 2013;61:931-44.

[26] Lu L, Garcia CA, Mikos AG. In vitro degradation of thin poly(DL-lactic-co-glycolic acid) films. J Biomed Mater Res 1999;46:236-44.

[27] Odelius K, Hoglund A, Kumar S, Hakkarainen M, Ghosh AK, Bhatnagar N, et al. Porosity and pore size regulate the degradation product profile of polylactide. Biomacromolecules 2011;12:120-1258.

[28] Peters R, Litvinov VM, Steeman P, Dias AA, Mengerink Y, van Benthem R, et al. Characteristics of UV-cured acrylate networks by means of hydrolysis followed by aqueous size-exclusion combined with reverse-phase chromatography. J Chromatography A 2007;1156:111-23.

[29] Ebenstein DM, Pruitt LA. Nanoindentation of biological materials. Nano Today 2006;1:26-33.

[30] Pedron S, Peinado C, Bosch P, Benton JA, Anseth KS. Microfluidic approaches for the fabrication of gradient crosslinked networks based on poly(ethylene glycol) and hyperbranched polymers for manipulation of cell interactions. J Biomed Mater Res Part A 2010;96:196-203.